Drew University

College of Liberal Arts

THE INFLUENCE OF mtDNA IN INNATE IMMUNE RESPONSES VIA THE cGAS-STING PATHWAY

A Thesis in Biology

By

Brenna Hezel

Advisor: Dr. Brianne Barker

Submitted in Partial Fulfillment of the

Requirements for a Degree in Bachelor of Science

with Specialized Honors in Biology

May 2026

Acknowledgments

This thesis is the culmination of my undergraduate journey, and it would not have been possible without the support, guidance, and encouragement of many individuals. I am incredibly fortunate to have had the following people in my corner throughout this process.

I would like to express my deepest gratitude to Dr. Brianne Barker. Your mentorship over the last four years at Drew—evolving from my freshman summer advisor to my academic advisor, Principal Investigator, and ultimately a cherished mentor and parental figure—has been invaluable. Thank you for sharing your expertise, for your tireless patience, and for pushing me to grow as a student, a researcher, and a woman. Words cannot fully express how indebted I am to you. Thank you for letting me be the Rocky to your Ryland Grace.

I am also deeply grateful to my Co-Principal Investigator, Dr. Stephen Dunaway. Thank you for constantly pushing me and challenging me to be better. Thank you for always having my back when it mattered most. While our journey included its fair share of ups and downs, I recognize now that those moments were essential to my growth. I truly would not be where I am today without you. Beyond the lab, knowing that you are always just a call away for advice or support means the world to me.

I am deeply grateful to Dr. Jessica McQuigg and Dr. Wendy Kolmar for their insightful feedback and academic support. If it were not for Dr. McQuigg, I would never have joined a research lab or envisioned my future as a scientist. Thank you for being a sister to me throughout this journey. Similarly, I owe a great debt to Dr. Kolmar, who provided me with a safe space to explore my passion for English Literature and my love for reading.

I also want to thank my family: my parents, Hope and Jeffrey, my siblings Michael, Paige, Grace, and Amanda, and my nephew Lukas. Being a part of our family has been the greatest honor of my life. Whether you were listening to my practice presentations or providing a much-needed distraction, your unwavering belief in me kept me moving forward. Sorry for talking all the time! Most importantly, thank you for watching me grow and for always encouraging me to be a better person—a better me. I could not have reached this milestone without you.

Finally, I am incredibly lucky to have spent my time at Drew surrounded by such a supportive community. To the members of the Barkaway Lab, thank you for making the lab feel like home. To my best friends, Emily Bass and Trinnawan Srisawang: thank you for being my constant source of joy and sanity. Whether we were decompressing after a long day or celebrating small wins, your friendship has been my anchor.

I am so grateful to have had all of you by my side throughout this journey.

Abstract

The innate immune response serves as the primary defense against microbial infection, triggered by the detection of Pathogen-Associated Molecular Patterns (PAMPs) by Pattern Recognition Receptors (PRRs). During viral infection, activation of the cGAS-STING pathway triggers a signaling cascade resulting in the production of Type I Interferons (IFNs) and the subsequent expression of Interferon-Stimulated Genes (ISGs) to establish an antiviral state. Although the recognition of RNA and DNA were long considered to occur via distinct pathways, recent investigations reveal that RNA virus infections can unexpectedly activate DNA-sensing proteins. This activation is driven by cellular stress and the leakage of mitochondrial DNA (mtDNA) into the cytosol, where it acts as a Damage-Associated Molecular Pattern (DAMP). Given that RNA viruses trigger mtDNA leakage after viral genome recognition, we hypothesize that DNA viruses employ a parallel mechanism where mtDNA is partially responsible for cGAS-STING activation.

To investigate this, we utilized a THP-1 cell model treated with ABT-737 and Q-VD-OPH to induce mtDNA release and prevent cell death. Using an adapted DNA fractionation protocol and reverse transcription quantitative real-time PCR (RT-qPCR), we confirmed that ABT-737 and Q-VD-OPH successfully trigger the transcriptional upregulation of ISGs and IFNs. Our initial results demonstrate that while total cellular DNA levels remain constant across all conditions, mtDNA leaks into the cytosol following viral DNA stimulation, lipid transfection, and the pharmacological treatment. This model provides a robust framework to decouple the sensing of exogenous viral DNA from endogenous mtDNA leakage, clarifying the specific contributions of each to the cGAS-STING response during DNA virus infection.

Table of Contents

Common Acronyms and Abbreviations

cDNA – Complementary DNA

cGAS – Cyclic Guanosine Monophosphate-Adenosine Monophosphate Synthase

cGAMP (Cyclic GMP–AMP) – Cyclic Guanosine Monophosphate–Adenosine Monophosphate

Cq – Quantification Cycle

DAMP – Damage-Associated Molecular Pattern

ER – Endoplasmic Reticulum

IFN – Interferon

IFNAR – IFN α/β receptor

ISG – Interferon-Stimulated Gene

IRF – Interferon Regulatory Factor

mtDNA – Mitochondrial DNA

NF-κB – Nuclear factor kappa-light-chain-enhancer of activated B cells

PAMP – Pathogen-Associated Molecular Pattern

PMA – Phorbol Myristate Acetate

PRR – Pattern Recognition Receptor

ROS – Reactive Oxygen Species

RT-qPCR – Reverse Transcription Quantitative Polymerase Chain Reaction

qPCR – Quantitative Polymerase Chain Reaction

RIG-I – Retinoic acid-inducible gene I

STING – Stimulator of Interferon Genes

TBK1 – TANK-Binding Kinase 1

Vac70 – Vaccinia Virus 70

Introduction

Background

The immune system is composed of cells, tissues, and organs responsible for defending the body against pathogens and maintaining physiological homeostasis. The system comprises two distinct branches: innate and adaptive (Parham 2021). The innate immune response acts as the first line of host defense and can be found across all multicellular organisms. In terms of time and purpose, this broad response is fast (minutes to hours) to protect the host from the surrounding environment in which a variety of toxins and infectious agents including bacteria, fungi, viruses and parasites are found. On the other hand, the adaptive immune response operates on a delayed timeline (days to weeks) as it develops a specialized defense to eliminate specific pathogens and establish long-term immunological memory. The adaptive immune system consists of two main cell types that drive two primary responses: B cells (which lead the antibody response) and T cells (which govern the cell-mediated response). While B cells handle threats in the bodily fluids, T cells directly attack infected host cells and coordinate the overall immune strategy (Parham 2021). The innate immune system differs from the adaptive by utilizing physical and anatomical barriers as well as immunological cells that detect, engulf, and destroy pathogens while signaling for backup. These white blood cells, referred to as leukocytes, include neutrophils, macrophages, dendritic cells, and natural killer cells. Our research specifically investigates the innate response during viral infection.

To defend the host against a virus, the immune system must halt the immediate infection and alert nearby cells. This protective state, referred to as the antiviral state, is defined as a specialized cellular condition where a cell has activated its internal defenses to block viral replication and prevent the spread of infection to neighboring cells (West et al. 2015). The

antiviral state allows a cell and its neighbors to focus their energy and efforts solely toward defense against the infectious cycle (Figure 1). This communication is facilitated by the secretion of interferons (IFNs), a type of cytokine. Cytokines are chemical signal proteins that orchestrate the immune system's response to pathogens and tissue damage by regulating the proliferation, activation, and migration of leukocytes to effectively manage inflammation and initiate recovery (Parham 2021). After a cell becomes infected with a virus, it will transcriptionally upregulate Type I IFNs like IFNα and IFNβ. These cytokines will then bind to the IFN α/β receptor (IFNAR) on nearby uninfected cells (Mogensen 2009). This binding event will result in the transcription and translation of several IFN-stimulated genes (ISGs) in these uninfected neighboring cells. ISGs, like ISG56, are a broad family of effector proteins that interfere with various stages of the viral life cycle including entry, genome replication, protein synthesis, and exit. This coordinated induction of ISGs transforms the local cellular environment into a hostile landscape for the pathogen, effectively stopping viral progression and providing the host with a critical window of time to mount a more specialized adaptive immune response.

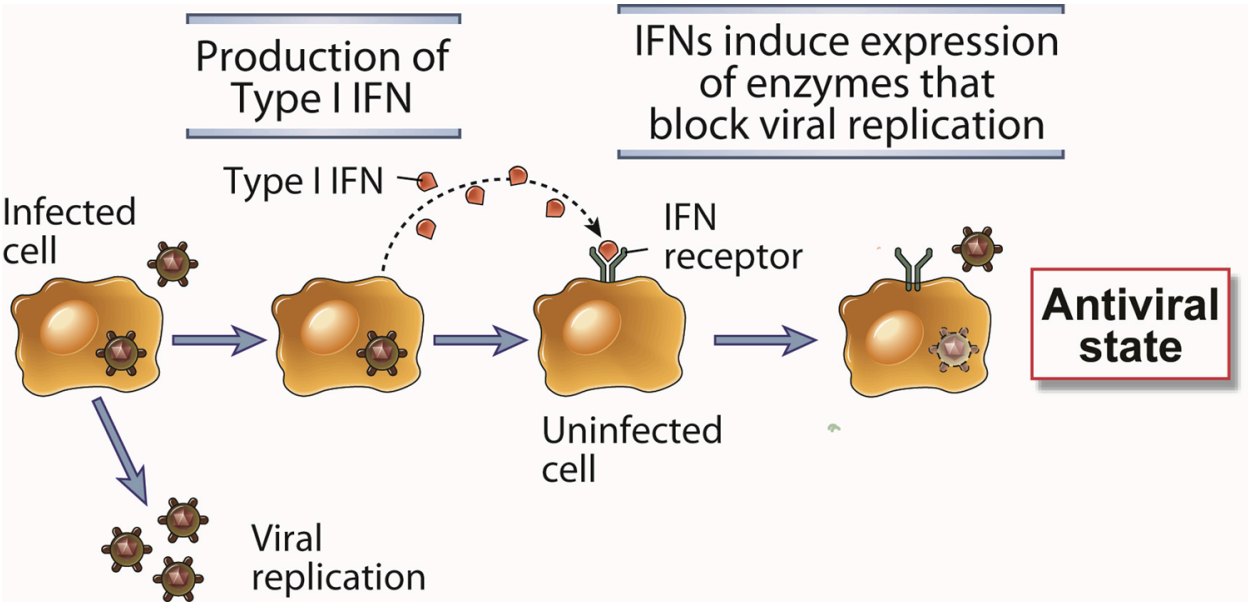

Figure 1: The Antiviral State. The antiviral state is a protective lockdown triggered when a cell detects a viral threat and releases warning signals called interferons (IFNs). These signals bind to nearby cells, prompting them to produce specialized proteins (ISGs) that "sabotage" the virus by interrupting entry, genome replication, protein synthesis, and exit in the viral cycle. This defense halts the spread of the infection to healthy tissue. Image adapted from Abbas *Cellular and Molecular Immunology* Fig. 4-15.

How does the infected cell know it is infected? Cells specifically utilize specialized pattern recognition receptors (PRRs) that bind to non-self-pathogen-associated molecular patterns (PAMPs). PAMPs are a broad class of foreign molecules including proteins, lipids, nucleic acids or other biological macromolecules (West and Shadel 2017). In addition to PAMPs, damage-associated molecular patterns (DAMPs) are also sensed by PRRs. DAMPs are molecules produced during stress conditions including those generated by physical, chemical, nutritional, biological, and metabolic stressors (Kanneganti et al. 2015). These danger signals activate the innate immune system to promote inflammation and tissue repair. While PAMPs are traditionally defined as exogenous molecules, DNA presents a unique challenge to immune discrimination. In a homeostatic state, host DNA is sequestered within the nucleus to protect the integrity of the genome. However, the mislocalization of DNA into the cytoplasm represents a critical biological danger signal typically associated with bacterial or viral infection. The host genome is strictly sequestered within the nucleus; therefore, the presence of cytosolic DNA serves as a definitive indicator of cellular compromise. This is recognized by the cGAS-STING pathway, a sophisticated sensing mechanism that detects these misplaced nucleic acids to initiate a robust inflammatory and antiviral response.

Initiation of the host antiviral response is contingent upon innate surveillance mechanisms; specifically, the cGAS-STING signaling pathway (Bryant et al. 2022). This pathway, a fundamental piece in innate immunity, allows cells to sense the presence of abnormal DNA in the cytoplasm (Figure 2). DNA is normally confined to specific compartments within the cell; however, it can be displaced into the cytosol under stressful conditions like viral infection, cellular stress, or cellular damage. Cyclic guanosine monophosphate–adenosine monophosphate synthase (cGAS) recognizes this DNA by binding to the sugar–phosphate

backbone of double-stranded DNA (Xia et al. 2025). As a sequence-independent sensor, cGAS is uninterested in sequence itself and only cares that DNA is physically present in the cytoplasm. After it recognizes the abnormal DNA, cGAS will synthesize the cyclic dinucleotide second messenger cyclic GMP–AMP (cGAMP). This begins a signal cascade in which cGAMP diffuses through the cytoplasm and binds to STING (Stimulator of Interferon Genes), which is located on the membrane of the endoplasmic reticulum (ER). Once activated, STING moves from the ER to the Golgi apparatus and recruits a protein called TBK1 (TANK-binding kinase 1). As a kinase, its job is to find other proteins and turn them on by adding a phosphate group to them. Therefore, TBK1 will phosphorylate Interferon Regulatory Factor 3 (IRF3). Phosphorylated IRF3 undergoes homodimerization, a process where two identical molecules undergo a conformational change that allows them to lock into a stable and active complex. The paired IRF3 molecules will move and bind to specific DNA sequences that act as “on" switches for the cell's immune defenses. These signals, like Type 1 Interferons, exit the cell to induce the antiviral state and coordinate downstream immune response. Like DNA viruses, RNA viruses can also activate host antiviral defenses. RNA viral genomes are biochemically different from DNA viral genomes and thus, are detected by their own specialized set of RNA-binding PRRs. The signaling from these receptors converges on the activation of TBK-1 and IRF3, like DNA PRRs, driving IFN production (Parham 2021). RNA and DNA sensing were traditionally treated as independent; however, we now know RNA viruses can trigger the cGAS-STING pathway via RNA and DNA sensors. The central mystery now lies in the relationship between these two systems.

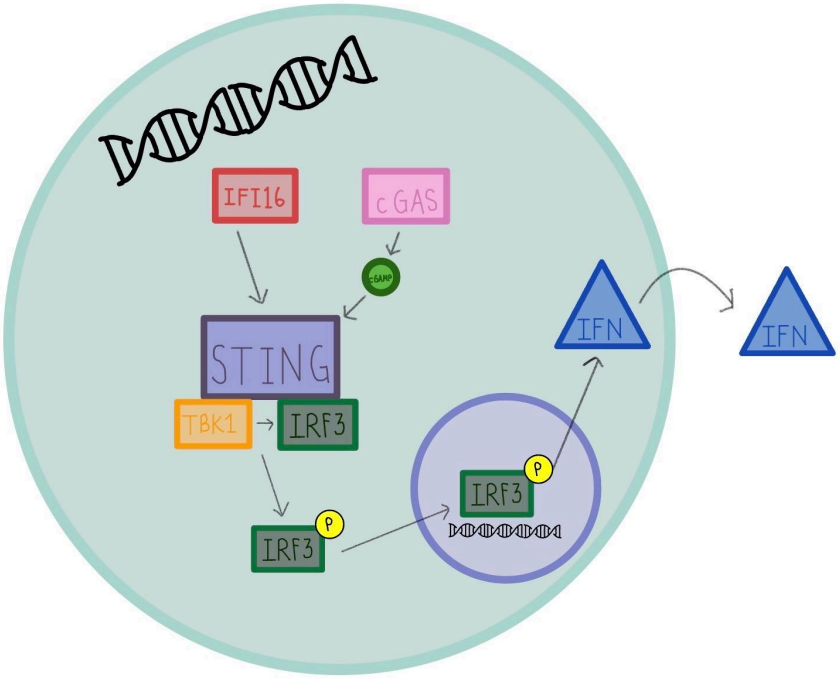

<u>Figure 2:</u> Activation of the cGAS-STING pathway via a viral DNA infection. Viral DNA is recognized by cytosolic sensors like cGAS. Activation of these sensors triggers the recruitment of downstream adaptors, STING, which undergo phosphorylation. These adaptors facilitate the recruitment of the kinases TBK1, leading to the phosphorylation and dimerization of IRF3. Following dimerization, IRF3 translocates to the nucleus to drive the transcription of Type I Interferons (IFNs). Image adapted from Emily Shirk in the Barkaway Lab.

Historically, it was once thought that RNA and DNA viral genomes were sensed exclusively by their corresponding nucleic acid sensors due to their biochemical differences. However, recent studies have demonstrated that DNA sensors are also critical for responding to RNA virus infections through indirect detection. For instance, despite being an RNA virus, Dengue triggers cellular damage that cGAS recognizes (Aguirre et al. 2017). Similarly, Norovirus utilizes a viral protein to trigger a displacement of host genetic material that activates the cGAS-STING and IFI16 pathways (Jahun et al. 2023). This activation in RNA viruses involves two main contributors: direct sensing of viral RNA by receptors, like retinoic acid-inducible gene I (RIG-I), and the sensing of cellular stress by DNA sensors (Amurri et al. 2023). What exactly is the cellular damage induced by these RNA viruses? RNA virus replication often triggers significant mitochondrial stress and the accumulation of reactive oxygen species (ROS), which compromises the integrity of the mitochondrial membrane. This physiological disruption leads to the release of mitochondrial DNA (mtDNA) into the cytosol, where it functions as an endogenous DAMP (VanPortfliet et al. 2024). This immune sensitivity to mtDNA is explained by the evolutionary history of the organelle. According to the endosymbiotic theory, mitochondria were their own prokaryotic cell that was engulfed by an ancestral eukaryotic cell (Lang et al. 1999). While most bacterial genes were eventually transferred to the host nucleus, a portion of the small circular genome was retained and became indistinguishable from foreign genetic material when it entered the cytosol. Since cGAS is a sequence-independent DNA sensor, it binds to this mislocalized mtDNA and catalyzes the production of the second messenger cGAMP, initiating the STING-dependent signaling cascade. It is also important to recognize that this pathway does not act in isolation. The resulting STING activation can further promote mitochondrial damage, creating a feedback loop that amplifies the

production of Type I IFNs and pro-inflammatory cytokines. Overall, host defense against RNA viruses is through DNA-sensing machinery to detect the cellular damage and RNA sensors to detect viral RNA genome. Given that RNA viruses trigger mtDNA leakage in addition to viral genome recognition, we hypothesize that DNA viruses employ a parallel mechanism where mtDNA is partially responsible for cGAS-STING activation.

Experimental Goals

The objective of this study is to determine if mtDNA is partially responsible for activating cGAS-STING during viral DNA infections. Studies have shown that viral RNA infections indirectly activate effectors, TBK1 and IRF3. This occurs when viral RNA recognition and subsequent cellular stress trigger the leakage of mtDNA into the cytosol (Hu et al., 2023). We hypothesize that the immune response employs a similar means for sensing DNA viruses. Viral DNA genome may be directly sensed by DNA sensors or, similar to viral RNA infections, result in the induction of cellular stress that triggers a secondary release of mtDNA. The experimental rationale designed to address if mtDNA is partially responsible for cGAS-STING activation during viral DNA infections is summarized in Figure 3.

To test this hypothesis, we first established a model system to induce and detect mtDNA leakage, as no such methodology previously existed in our laboratory. THP-1 cells were cultured, transfected, and treated with ABT-737 (a BCL-2 inhibitor) and Q-VD-OPH (a pan-caspase inhibitor) to induce mtDNA release while blocking apoptosis and necrosis. While apoptosis is typically a "quiet" programmed death and necrosis is a "loud" inflammatory death, this dual-drug approach induces mitochondrial damage and prevents both cell death types. ABT-737 blocks the BCL-2 proteins that normally shield the mitochondria, triggering mitochondrial permeabilization. Q-VD-OPH inhibits the downstream caspase enzymes responsible for the

death process. Following an adapted DNA fractionation protocol to isolate cytosolic mtDNA, transcriptional responses of *IFNβ* and *ISG56* were assessed via Quantitative Polymerase Chain reaction (qPCR) across four groups: untreated, mock-transfected, DNA-stimulated, and drug-treated. These experiments establish a protocol to determine the extent of mtDNA contribution in cGAS–STING activation during viral DNA infection.

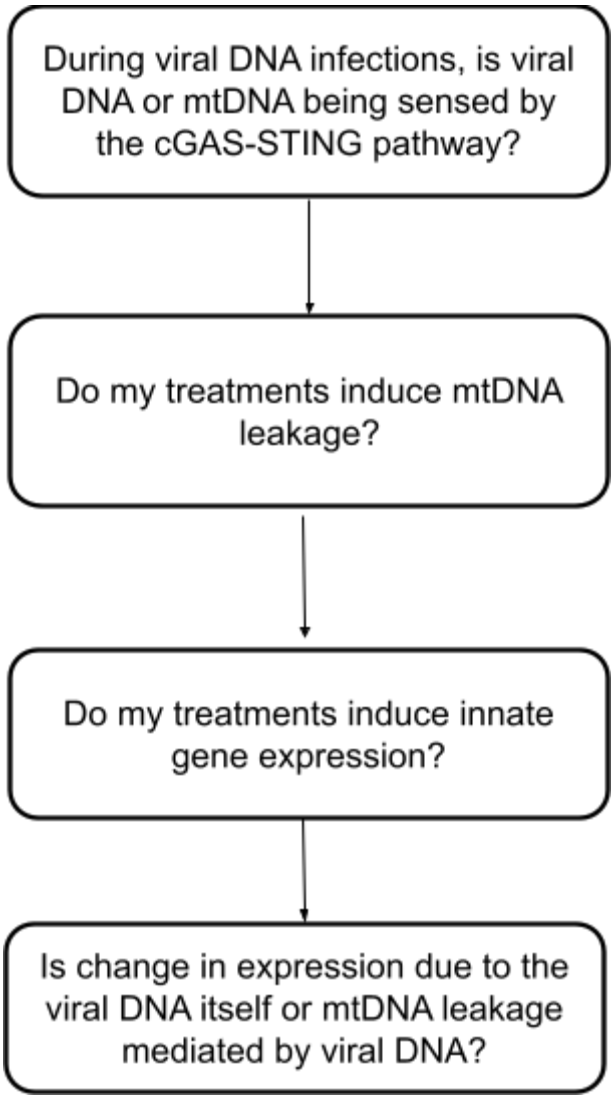

Figure 5: Experimental Flowchart: This flowchart details the rationale for the order of experiments conducted in this study to answer the study's objective.

Methods

Cell Culture

THP-1 cells (from ATCC) were cultured in R10 medium (RPMI media (Gibco), 10% fetal bovine serum (Gibco), 5 mL/500 mL penicillin-streptomycin-glutamine (PSG, from Invitrogen), 5 mL/500 mL sodium pyruvate (Invitrogen), 5 mL/500 mL HEPES buffer (Gibco), and 5 mL/500 mL 7.5% sodium bicarbonate (Gibco)). Cells were incubated overnight at 37°C and 5% CO_2.

Cell Stimulation

Before each experiment, cells were plated in a 6 well plate to create a concentration of $2x10^6$ cells in 3 mL of R10. While THP-1 cells resemble undifferentiated human monocytic cells (Tsuchiya et al. 1980); they can be matured into a macrophage-like phenotype characterized by widespread proteomic changes. To induce this maturation, cells were treated with 5ng/mL of phorbol myristate acetate (PMA) followed by 72 hours of incubation (Yoh et al. 2015).

Cell stimulations were performed through 10 µL of Lipofectamine 2000 (Invitrogen) mixed with 240 µL of Opti-MEM (Invitrogen), a buffered, simplified form of media. For viral DNA stimulation, 246 µL of Opti-MEM (Invitrogen) and 4 µL of nucleic acid for a final concentration of 1.33 µg/mL was mixed. Both mixtures were incubated at room temperature for 5 minutes. After incubation, both mixtures were combined and incubated at room temperature for 20 minutes to 6 hours before addition to the cells, as per the manufacturer's instructions. The mock-transfected treatment ("Mock") samples were generated by combining the Lipofectamine 2000 mixture with pure Opti-MEM while the untreated samples ("Unstim") were prepared without Opti-MEM, lipofectamine, or nucleic acid. A mock treatment was used to compare the

effects of lipid transfection via Opti-Mem because the viral DNA-stimulated cells ("DNA") received a combination of the Lipofectamine 2000 mixture, Opti-MEM, and Vac70. Vac70 (Invitrogen) is 70 base pairs of DNA from the genome of Vaccinia virus that is known to induce IFN in a STING-dependent manner (Unterholzner et al. 2010). DNA stimulation was used at a concentration of 2 μg DNA/mL of cells. Our positive control drugs ("Drugs"), Q-VD-OPH and ABT-737, were delivered together from 3 μL of a 10mM stock each. The negative control used in this experiment was referred to as "unstimulated" because nothing was added to the cells after they were cultured overnight. All reactions were incubated for the indicated times (or overnight if not indicated) in the media at 37°C and 5% CO_2 after stimulation.

mtDNA Methodology

To investigate the role of mtDNA in innate immune DNA sensing, a published fractionation protocol was adapted and employed to isolate and analyze DNA from distinct cellular compartments. Traditional methods, like the Zymo Quick-RNA MiniPrep, will lyse the cell and prevent fractionation. Therefore, this protocol uses a gentle detergent-based method to fractionate (Bryant et al. 2022). The three buffers, including SDS, Digitonin, and NP-40, allow us to cleanly isolate cytosolic, mitochondrial, nuclear, and whole cell extracts.

Following fractionation, the DNA from each fraction was isolated using a phenol/chloroform/isoamyl alcohol extraction and ethanol precipitation. First, for each 400 μL DNA sample, 2 μL of 5 mg/mL RNase A was added and incubated at 37 °C for 1.5 hours. Second, 4 μL of 20 mg/mL proteinase K was added and samples incubated at 55 °C for 1 hour. RNase A degrades RNA, while proteinase K degrades any residual proteins. Third, an equal

volume of 400 μL of phenol/chloroform/isoamyl alcohol was added, vortexed vigorously for 1 minute, and centrifuged at maximum speed for 5 minutes at room temperature. Next, the aqueous layer was removed and further purified through the addition of 320 μL of chloroform/isoamyl alcohol. Precipitation occurs thereafter from the mixture of 28 μL of NH_4OAc, 1 μL of glycogen (20 μg), and 697.5 μL of ethanol. DNA is specifically precipitated at -80 °C for 1 hour and forms a pellet from centrifugation. Finally, a 95% ethanol wash occurred twice and samples were left out to dry so the pellets could be resuspended in 20 μL of TE buffer for nanodropping and qPCR analysis. A simplified diagram of the adapted methods can be seen in Figure 3.

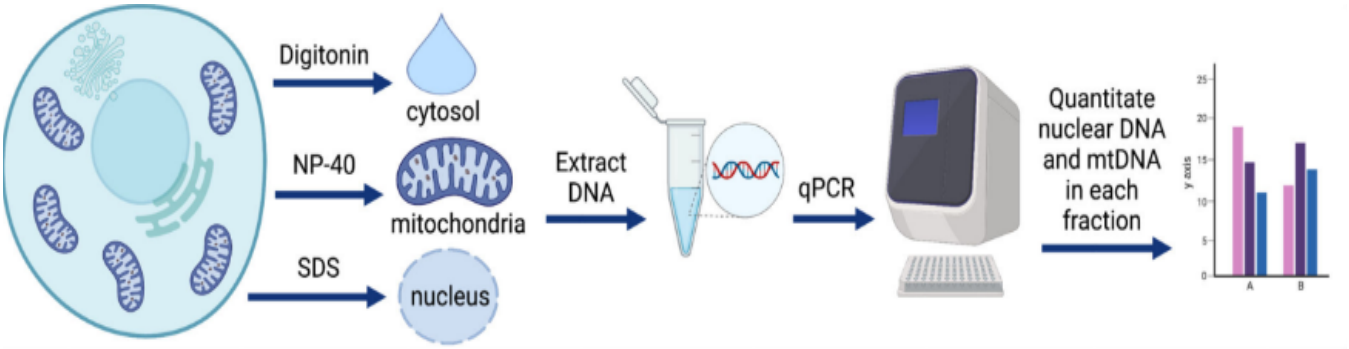

Figure 3: Process of mtDNA compartmentalization and extraction. This protocol and figure are adapted from Bryant 2022. Methodology includes compartmentalizing and extracting 4 DNA samples. Primers used during qPCR allow us to determine how much nuclear or mtDNA is in that specific compartment

Extracted DNA samples were then diluted to 50 µL of a 2ng/µL solution for each sample. For quantitative PCR analysis, 4.5µL of samples were mixed with 5µL iTaq Universal SYBR Green mix, 10µL nuclease-free water, and 0.25 µL (500 nM stock solutions) each of the forward and reverse primers. Using the SYBR Green-based qPCR methodology, validated primers were selected for each compartment. These protocols only require whole cell and cytosolic extracts. *KCNJ10* acted as a nuclear DNA control and *MT-D-Loop* amplified mtDNA. Primer sequences for mtDNA extraction and isolation are in Table 1.

<u>Table 1:</u> Primers for mtDNA extraction and isolation protocols

Primer	**Reverse or Forward**	**Sequence**
KCNJ10	Forward	5’-GCG CAA AAG CCT CCT CAT T-3’
KCNJ10	Reverse	5’-CCT TCC TTG GTT TGG TGG G-3’
MT-D-Loop	Forward	5’-CCG TGA GTG GTT AAT AGG GTG ATA -3’
MT-D-Loop	Reverse	5’-CCG TGA GTG GTT AAT AGG GTG ATA-3’

To accurately quantify mtDNA release into the cytosol, ΔΔCq methods were adapted in order to quantify qPCR data from whole cell and subcellular fractions. The whole Cell ΔCq was calculated to establish the baseline ratio of mitochondrial DNA to nuclear DNA, effectively measuring the total mitochondrial load per cell. To visualize these distributions, we employed the ΔΔCq method, normalizing the whole-cell samples against themselves to create a reference value of 1.0. This allowed us to quantify the mtDNA compartmentalization by comparing the abundance of mtDNA in specific fractions relative to the total cellular pool. By analyzing the cytosolic fraction, we were able to determine if mtDNA translocation had occurred, indicating whether mitochondrial DNA had leaked out of the organelle and into the cytoplasm. The calculations, adapted from Bryant et al. are as follows.

Equation 4: Whole Cell Extracts Calculation

$$\Delta Cq = Cq\ (\textit{MT-D-Loop}) - Cq\ (\textit{KCNJ10})$$

$$\Delta\Delta Cq = \Delta Cq - \text{Avg. } \Delta Cq \text{ Mock}$$

$$\text{Fold Change} = 2^{-\Delta\Delta Cq}$$

Equation 5: Cytosolic Extracts Calculation

$$\Delta Cq = Cq\ (\textit{MT-D-Loop} \text{ in Cytosol Extract}) - \Delta Cq\ (\text{Whole Cell Extract})$$

$$\Delta\Delta Cq = \Delta Cq - \text{Avg. } \Delta Cq \text{ Mock}$$

Innate Gene Expression Methodology

Measurements of *IFNβ* and *ISG56* transcription levels were from samples lysed and RNA extracted according to the protocol of the Zymo Quick-RNA MiniPrep Kit (obtained from Zymo Research). After RNA was extracted, nucleic acid concentration and purity were confirmed via Nanodrop from 2 μL of each sample and finally stored at -80°C. Purity was determined based on peaks in the spectrometer: a peak at 270 indicates nucleic acid. If there was a peak at 230 then there was contamination from the solvent. If there was a peak at 280, then that indicates protein contamination. Complementary DNA (cDNA) was prepared thereafter according to the protocol of the ProtoScript First Strand cDNA Synthesis Kit (obtained from New England BioLabs) and stored at -20°C. To produce cDNA, each RNA sample was either normalized to 1000 ng or 6 μL. RNA amounts added during cDNA synthesis were controlled to ensure that every sample in an experiment was made using the same amount of RNA. A simplified diagram of methods can be seen in Figure 4.

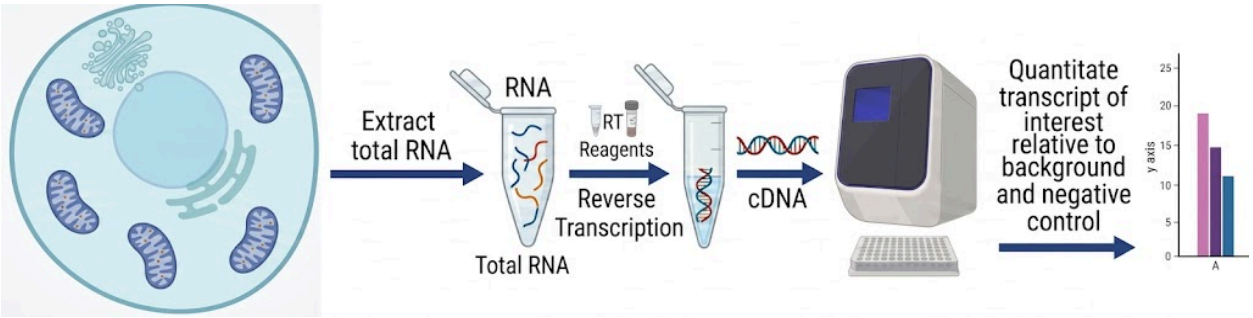

<u>Figure 4:</u> Process of RNA extraction and Innate Gene Expression Experiment. Methodology includes extracting RNA then making cDNA through reverse transcriptase. Primers used during RT-qPCR allow us to determine how much gene expression is related to the control there is.

For Reverse Transcription Quantitative Polymerase Chain Reaction (RT-qPCR) analysis, 2 µL of cDNA samples were mixed with 10µL iTaq Universal SYBR Green mix, 6µL nuclease-free water, and 1µL each of forward and reverse primers (500 nM stock solutions). The primary difference between qPCR (used in the mtDNA experiment) versus RT-qPCR (in the innate gene expression experiment) is the starting material. qPCR measures DNA directly, whereas RT-qPCR uses the enzyme reverse transcriptase to first convert RNA into cDNA so that transcription levels can be measured. The transcription of the housekeeping gene, *RPL37A*, was measured to determine background transcription levels in the cell. *RPL37A*, specifically, encodes a protein of a ribosomal subunit and was selected because it is expressed at similar levels across our cell type nor is its expression influenced by our stimuli (Popovici et al. 2009; Maess et al. 2010). The other two primers were selected to amplify *ISG56* and *IFNβ*. The primers for the genes of interest were obtained from IDT and sequences (Table 2).

<u>Table 2:</u> Primers used in qPCR of IFNβ, ISG56, and RPL37A

Primer	**Reverse or Forward**	**Sequence**
ISG56	Forward	5’-CCT CCT TGG GTT CGT CTA CA-3’
ISG56	Reverse	5’-GGC TGA TAT CTG GGT GCC TA-3’
IFNβ	Forward	5’-CAC GCT GCG TTC CTG CTG TG-3’
IFNβ	Reverse	5’-AGT CCG CCC TGT AGG TGA GGT T-3’
RPL37A	Forward	5’-ATT GAA ATC AGC CAG CAC GC-3’
RPL37A	Reverse	5’-AGG AAC CAC AGT GCC AGA TCC-3’

Samples were run on Bio-Rad CFX96 qPCR machine for 40 cycles. Before cycling began, there was a 3-minute 95°C initial denaturation. One cycle consisted of a 10 second 95°C denaturation step followed by a 30 second 60°C annealing and elongation step. After 40 cycles, the machine went from 65°C to 95°C in 0.5°C increments and generated melt curves to confirm products.

Quantification Cycle (Cq) values from RT-qPCR were collected using SYBR Green fluorescence and normalized to the housekeeping gene *RPL37A*. To determine relative quantification, data was normalized to unstimulated (mock) samples to calculate fold change. Cq values are inversely proportional to the amount of target DNA, this calculation effectively measures the relative abundance of RNA across treatment groups. By setting the mock-transfected control to a baseline of 1, the resulting graph bars represent the magnitude of gene induction or suppression relative to the control. All data are representative of biological triplicates. Equation 1, 2, and 3 are as follows.

Equation 1: ΔCq Calculation

$$\Delta Cq = Cq \text{ of ISG56} - Cq \text{ of RPL37A}$$

Equation 2: ΔΔCq Calculation

$$\Delta\Delta Cq = \Delta Cq \text{ of experimental sample - AVERAGE } \Delta Cq \text{ negative control}$$

Equation 3: Fold Change Calculation

$$\text{Fold Change} = 2^{-(\Delta\Delta Cq)}$$

Statistical Analysis and Interpretation

The objective of this study was to determine if mtDNA is partially responsible for activation of the cGAS–STING pathway during viral DNA infections. For any methodological experiments, experiments conducted to establish standardized procedures, technical replicates were averaged to determine the mean and standard deviation. In some experiments, technical replicates were first averaged within each biological replicate. Biological replicates consist of independent cell treatments performed in separate wells of a 6-well plate. Technical replicates refer to the repeated qPCR measurements of a single biological sample to ensure the precision of the quantification. Regardless of type of replicate, values are used to calculate the overall mean and standard deviation across independent experiments. In certain experiments with *IFNβ* and *ISG56* gene expression following DNA and drug treatments (based on if there were enough biological and technical replicates), statistical significance was determined using a one-sample t-test. Specifically, treatment groups were compared against a theoretical fold change of 1.0, representing the baseline expression of the untreated control. Statistical significance was defined by a p-value less than 0.05 ($p < 0.05$), indicating that the DNA and drug treatments were significantly different from the untreated negative control.

Results

To address whether viral DNA-mediated mtDNA leakage activates the cGAS-STING pathway, we first sought to confirm the presence of mtDNA leakage. Using an adapted fractionation protocol, we measured mtDNA levels in both whole-cell and cytosolic extracts. This initial mtDNA extraction and compartmentalization experiment revealed that none of the treatments significantly altered the total mtDNA content in whole-cell extracts (Figure 5). However, a slight decrease in total mtDNA from the drug treatment was observed in several trials. We also confirmed that mtDNA leaked into the cytosolic fraction following both viral DNA stimulation and the positive control treatment (Figure 6). While the mock treatment caused a slight induction of mtDNA leakage compared to unstimulated cells, the overall results validate the protocol and demonstrate that viral DNA infection successfully triggers mtDNA release.

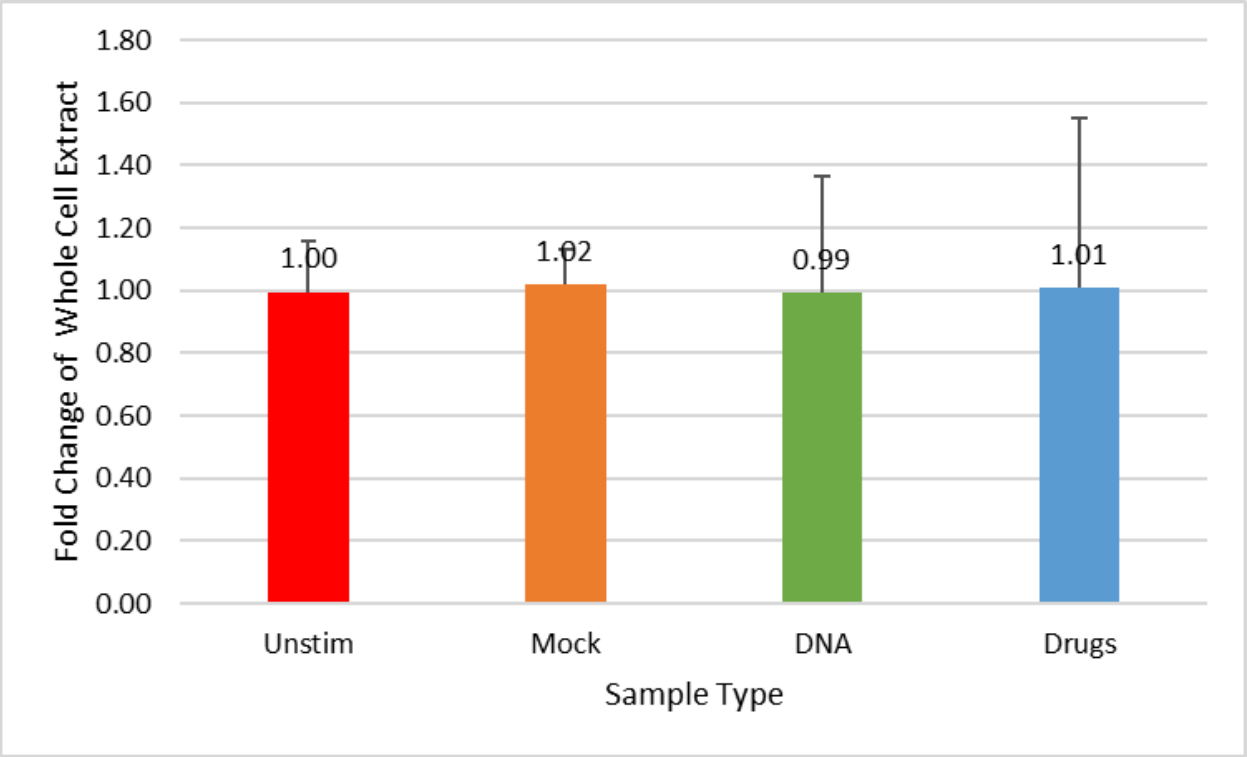

<u>Figure 5:</u> Compartmentalization and Extraction of DNA in the Whole Lysates.

PMA-treated THP-1 cells stimulated with Vac70 DNA, Lipofectamine with Opti-MEM, and the positive controls (Q-VD-OPH and ABT-737). Extraction and compartmentalization of DNA was adapted from Bryant et al. 2022. Measurements were taken 24 hours after stimulation. Data are representative of the mean of technical triplicates from three experiments, and error bars represent the standard deviation. This experiment was successfully repeated 3 times, each trial shared similar results.

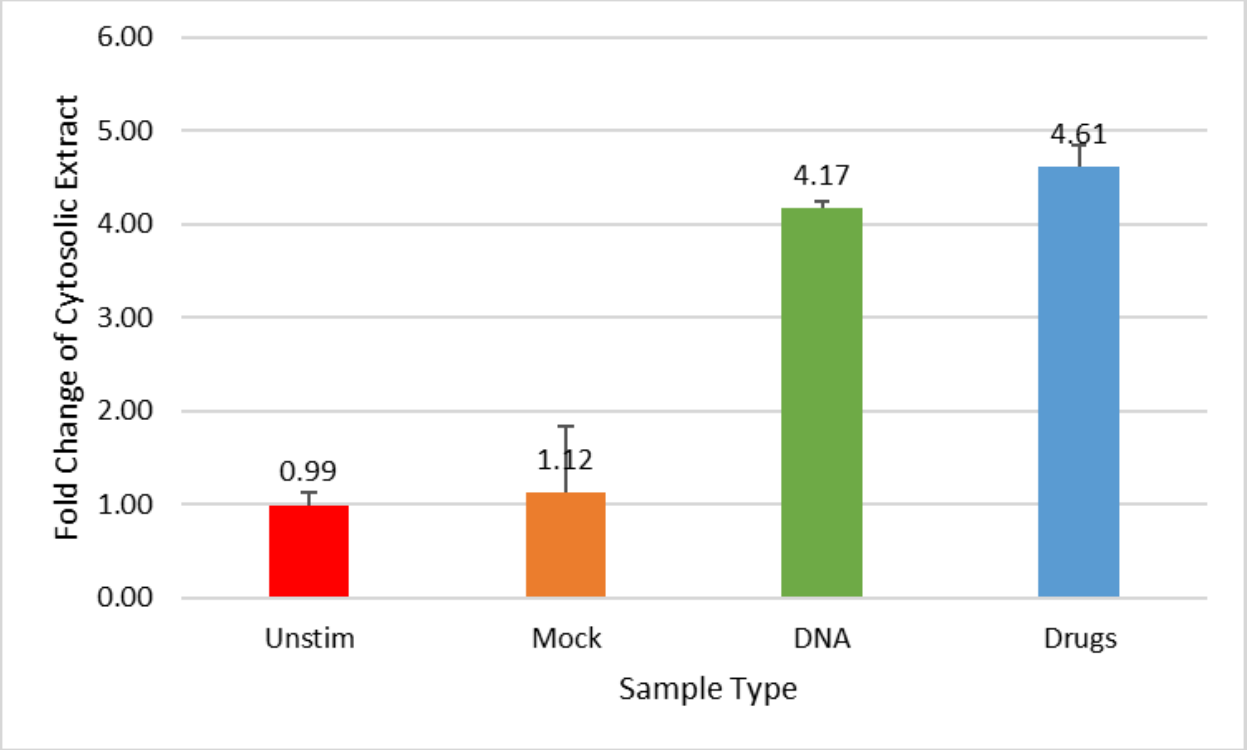

Figure 6: Compartmentalization and Extraction of DNA in the Cytoplasm. PMA-treated THP-1 cells stimulated with Vac70 DNA, Lipofectamine with Opti-MEM, and the positive controls (Q-VD-OPH and ABT-737). Extraction and compartmentalization of DNA was adapted from Bryant et al., 2022. Measurements were taken 24 hours after stimulation. Data are representative of the mean of technical triplicates from three experiments, and error bars represent the standard deviation. This experiment was successfully repeated 3 times, each trial shared similar results.

One of the interesting things about these drugs, Q-VD-OPH and ABT-737, is that they have not been used in an innate gene expression experiment. Therefore, the relationship between innate gene expression and experimental treatments had to be verified and the protocols, similar to the mtDNA experiment, had to be established. The treatments referred to include unstimulated cells, mock-lipid transfection, Vac70 DNA transfection, and experimental drug treatment. First, the optimal stimulation window for mtDNA and viral infection experiments had to be determined. In a 24-hour kinetics experiment, expression of *IFNβ* (Figure 7) and *ISG56* (Figure 8) were quantified using qPCR. Time zero acted as the baseline comparison of innate gene expression. The data indicates *IFNβ* expression peaks between 6 to 8 hours, while *ISG56* expression peaks between 12 to 24 hours post stimulation. The data aligns with current knowledge in the field surrounding signaling pathways and the fact that Type I IFNs induce the expression of ISGs (Parham 2021). Further kinetics analysis was conducted; specifically, a comparative analysis of 24-hour versus 48-hour stimulation in *IFN* (Figure 9) and *ISG56* (Figure 10). Based on these kinetics' experiments, a 24-hour post-stimulation point was selected for all subsequent extractions. Twenty four-hour post stimulation was selected for practicality and also because similar kinetics between the genes of interest were observed. These results further confirm that viral DNA and the positive control treatment led to increased expression of *IFNβ* and *ISG56*.

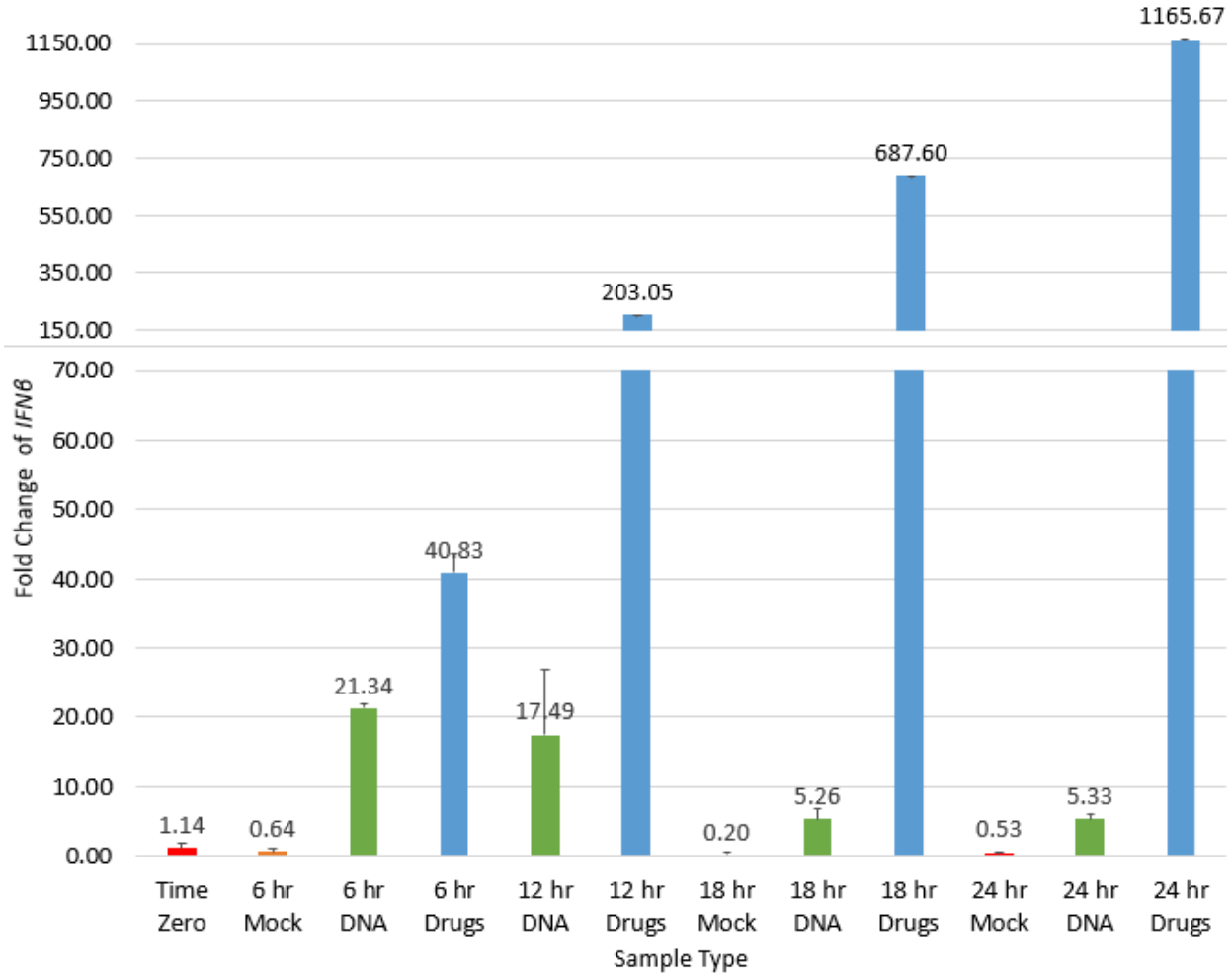

Figure 7: Kinetics of the cellular IFN response up to 24 hours. PMA-treated THP-1 cells stimulated with Vac70 DNA, Lipofectamine with Opti-MEM, and the mtDNA release drugs (Q-VD-OPH and ABT-737). Measurements were taken every 6 hours after stimulation. Data are representative of the mean of technical triplicates from three experiments, and error bars represent the standard deviation.

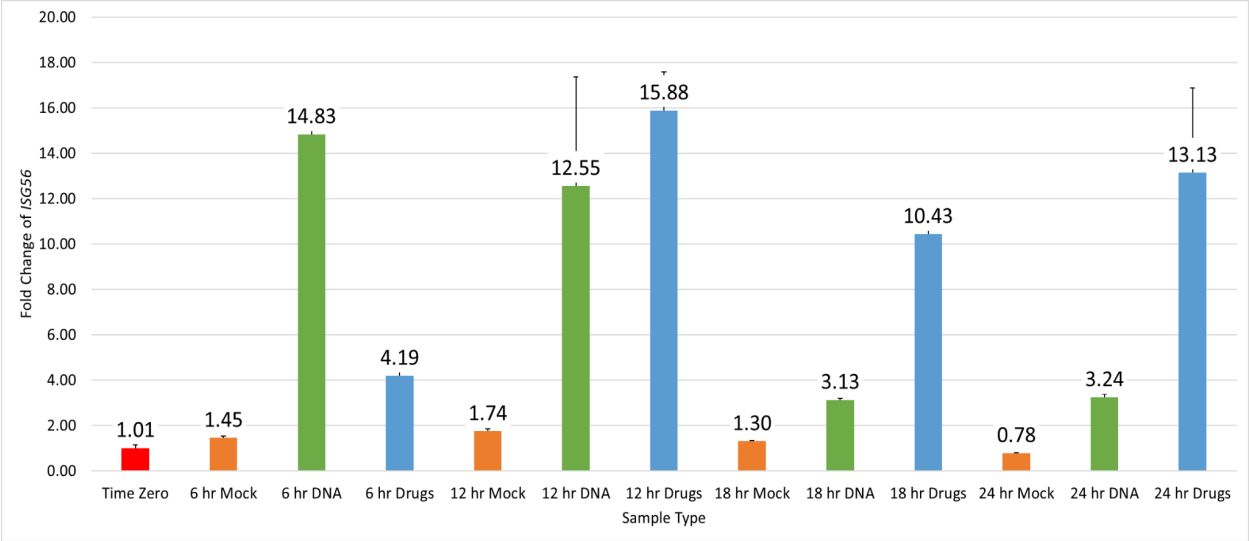

Figure 8: Kinetics of *ISG56* up to 24 hours. PMA-treated THP-1 cells stimulated with Vac70 DNA, Lipofectamine with Opti-MEM, and the mtDNA release drugs (Q-VD-OPH and ABT-737). Measurements were taken every 6 hours after stimulation. Data are representative of the mean of technical duplicate from three treatments, and error bars represent the standard deviation.

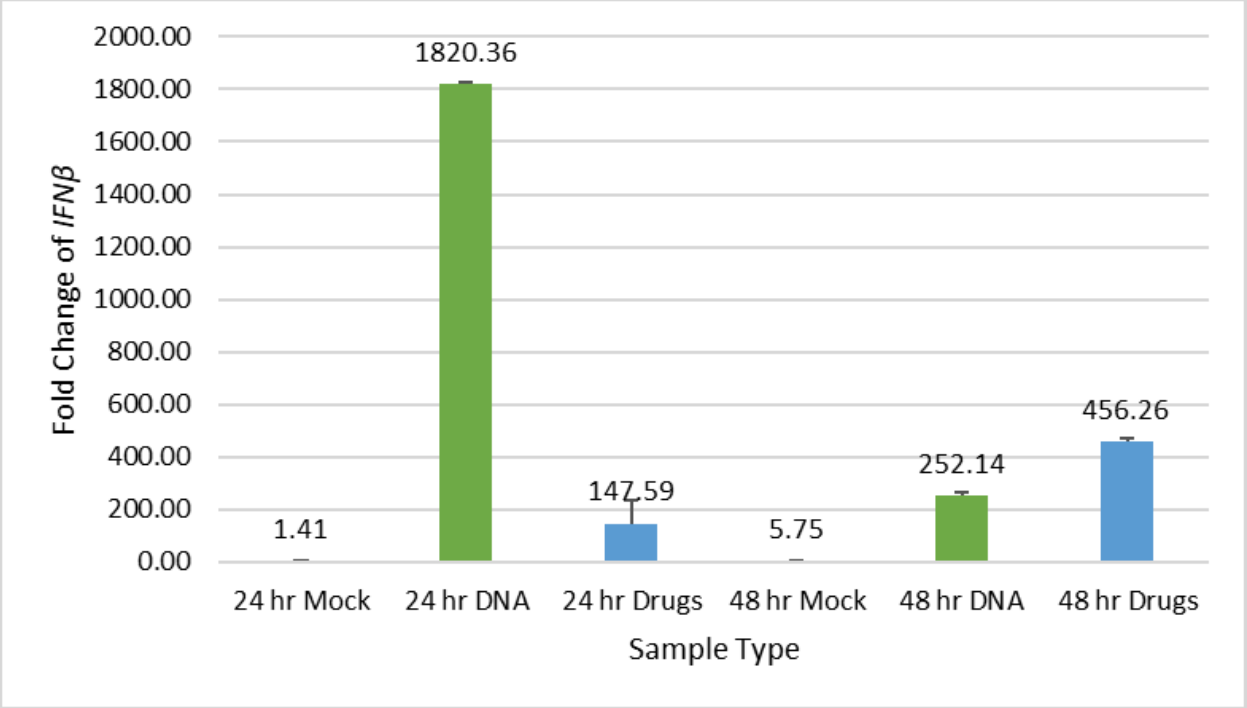

Figure 9: 24 hours versus 48 hours kinetics of *IFN*□. PMA-treated THP-1 cells stimulated with Vac70 DNA, Lipofectamine with Opti-MEM, and the mtDNA release drugs (Q-VD-OPH and ABT-737). Measurements were taken every 6 hours after stimulation. Data are representative of the mean of technical triplicates from three experiments, and error bars represent the standard deviation.

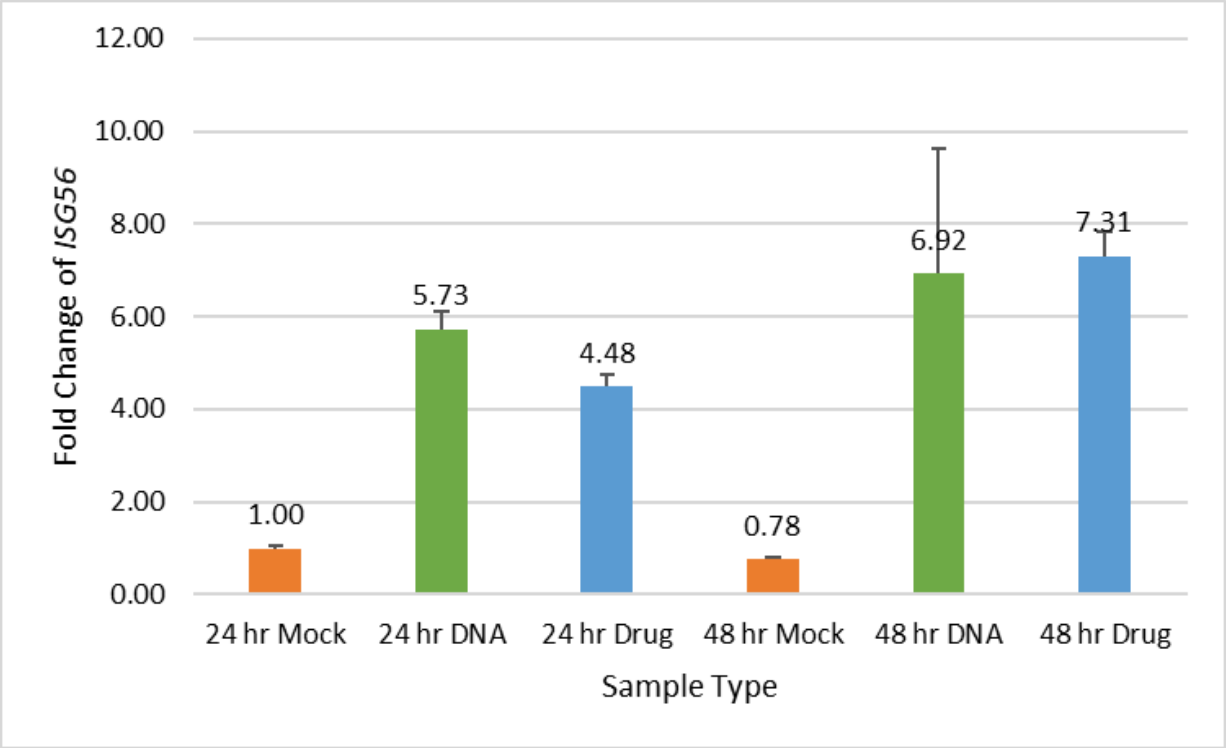

Figure 10: 24 hours versus 48 hours kinetics of *ISG56*. PMA-treated THP-1 cells stimulated with Vac70 DNA, Lipofectamine with Opti-MEM, and the mtDNA release drugs (Q-VD-OPH and ABT-737). Measurements were taken every 6 hours after stimulation. Data are representative of the mean of technical triplicates from three experiments, and error bars represent the standard deviation.

Following the 24-hour versus 48-hour kinetics trial, the 24-hour time point was applied to further qPCR transcriptional analysis of *IFNβ* (Figure 11) and *ISG56* (Figure 12). Both DNA and drug treatments resulted in a statistically significant increase in *IFNβ* fold change compared to mock (DNA: $df = 2$, $t = 4.37$, $p = 0.049$; Drug: $df = 2$, $t = 4.43$, $p = 0.047$). Likewise, both DNA and drugs treatments significantly increased *ISG56* fold change compared to mock (DNA: $df = 2$, $t = 4.86$, $p = 0.040$; Drug: $df = 2$, $t = 7.37$, $p = 0.018$). These data points were consistent with the kinetics data and the initial pilot study: both viral DNA and the positive control treatment resulted in increased expression of *IFNβ* and *ISG56* relative to the negative control. Furthermore, the expression levels by viral DNA were lower than the expression levels by the positive control treatment.

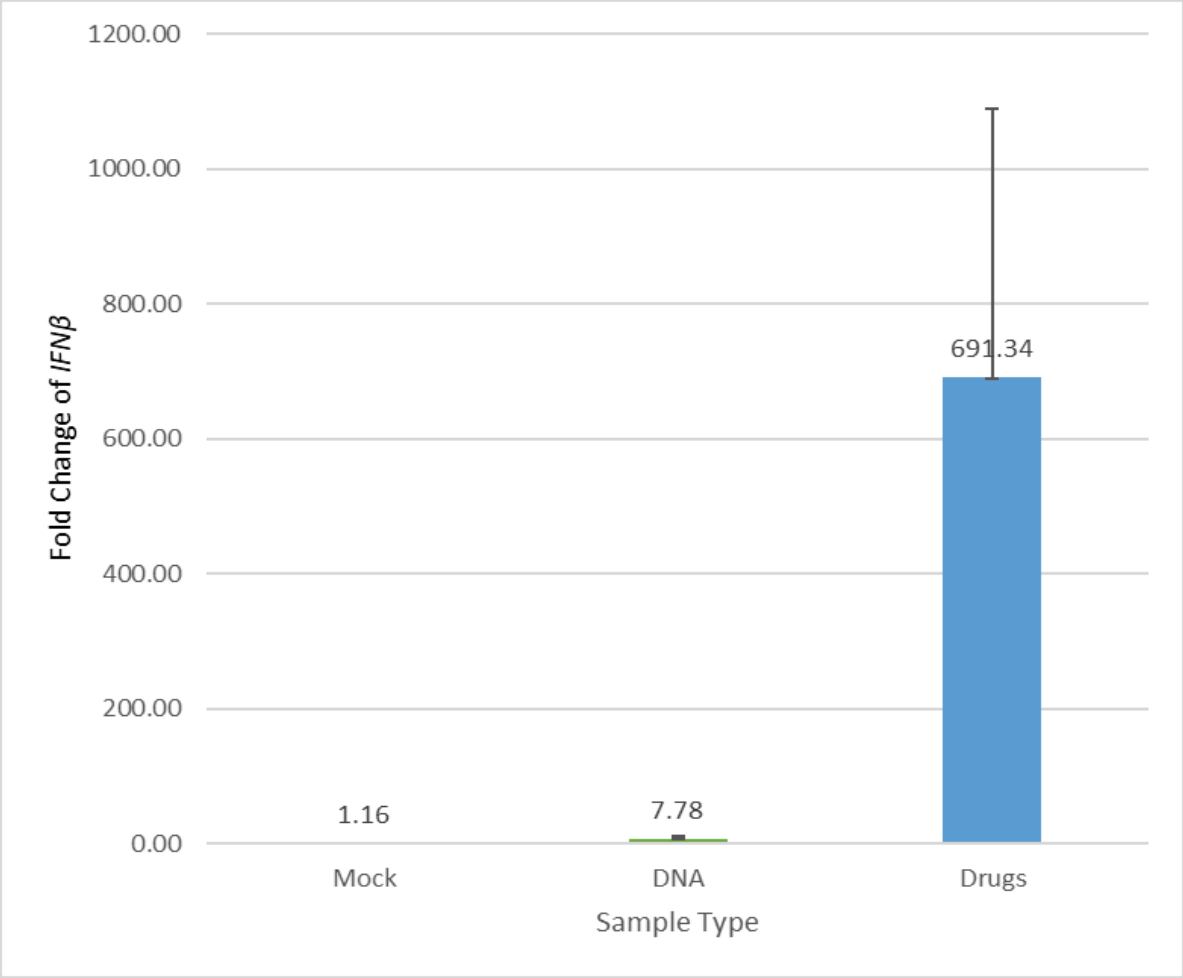

Figure 11: Transcription of *IFN*□ under mock lipid transfected, viral DNA, and mtDNA release drugs. PMA-treated THP-1 cells stimulated with Vac70 DNA, Lipofectamine with Opti-MEM, or the mtDNA release drugs (Q-VD-OPH and ABT-737). Measurements were taken 24 hours after stimulation. Data bars represent the three replicate wells that were pseudo replicated and have been averaged together. The error bars represent the standard deviation among the pseudo replicates. The third triplicate of the mock treatment was removed as results were inconclusive due to standard deviation. **DNA: df = 2, t = 4.37, p = 0.049; Drug: df = 2, t = 4.43, p = 0.047

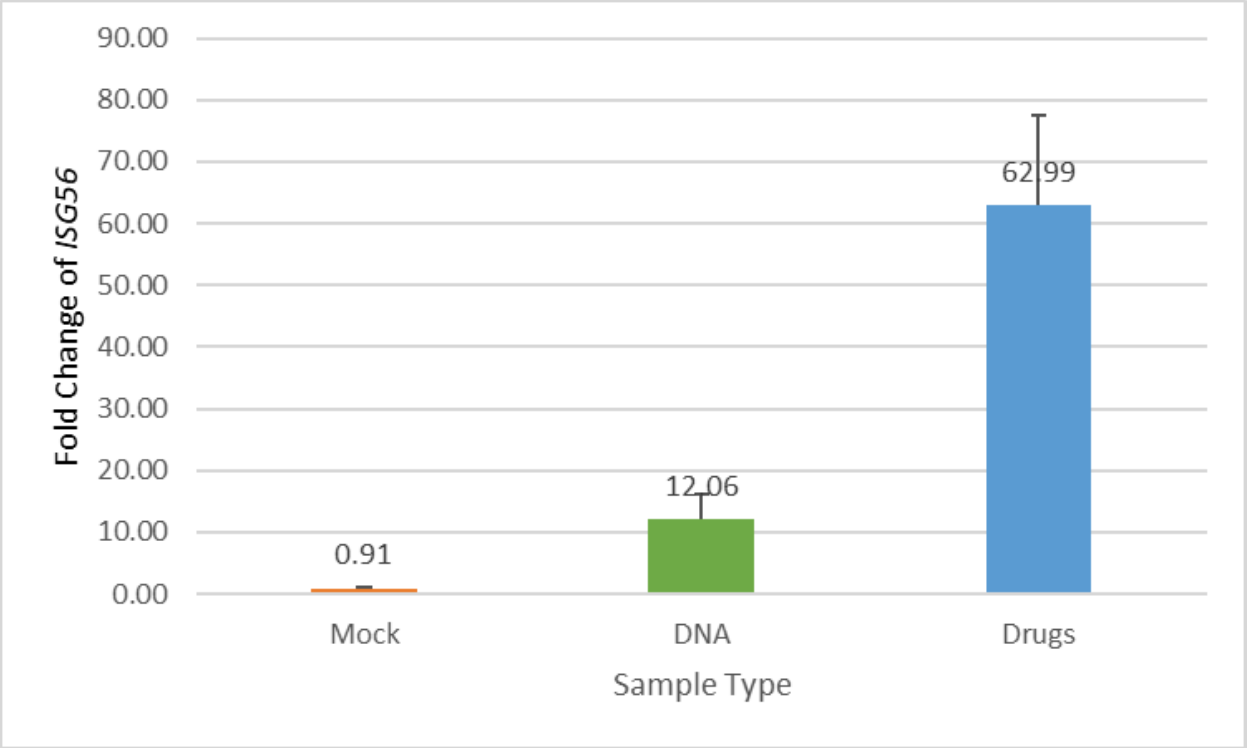

Figure 12: Transcription of *ISG56* under mock lipid transfected, viral DNA, and mtDNA release drugs. PMA-treated THP-1 cells stimulated with Vac70 DNA, Lipofectamine with Opti-MEM, or the mtDNA release drugs (Q-VD-OPH and ABT-737). Measurements were taken 24 hours after stimulation. Data bars represent the three replicate wells that were pseudo replicated and have been averaged together. The error bars represent the standard deviation among the pseudo replicates. The third triplicate of the mock treatment was removed as results were inconclusive due to standard deviation. **DNA: df = 2, t = 4.86, p = 0.040; Drug: df = 2, t = 7.37, p = 0.018

Our lab specifically utilizes a liposomal-based transfection reagent, in which a mixture of Lipofectamine and Opti-MEM enables the formation of positively charged lipid aggregates that can merge smoothly with the phospholipid bilayer of the host cell to allow the entry of the foreign genetic materials with minimal resistance (Kim and Eberwine 2010). Initial results from the mtDNA extraction experiment (Figure 5 and 6) with the kinetics experiment with time zero (Figure 9 and 10) indicated that this liposomal-based transfection increased expression of *IFN*□ and *ISG56.* At this point in the study, it was unclear whether the lipid was inducing activation of the cGAS-STING pathway. It was also an unequal comparison because the drug treatment does not include lipids, whereas the DNA treatment does. Therefore, it was decided that an evaluation of possible negative controls would be conducted.

Following standard RNA extraction and cDNA synthesis protocols, various combinations of lipid reagents were evaluated to observe IFNβ expression via RT-qPCR (Figure 13). Due to the relationship between IFNβ and ISG56 observed in previous experiments, only IFNβ was assessed. Experimental conditions included "Mock Lipo" (Lipofectamine 2000), “Vac” (Vac70 with a lipid), and "F" (an alternative reagent referred to as Fusion) or "LyoVec" (another alternative lipid reagent). To determine if the response was driven by concentration or the lipid composition itself, we compared different manufacturing preparations: "R" (the manufacturer-recommended concentration) and "No R" (a concentration adjusted to match Lipofectamine levels). "Untreated" samples served as the baseline control. Notably, both "Untreated" and "Mock" conditions exhibited similar baseline expression, while "Vac" and "LyoVec" groups showed increased induction. “F” showed an extreme increase in induction. To

maintain consistency, "untreated" samples were defined as the negative control for all subsequent experiments. Future experiments may want to further investigate these lipids.

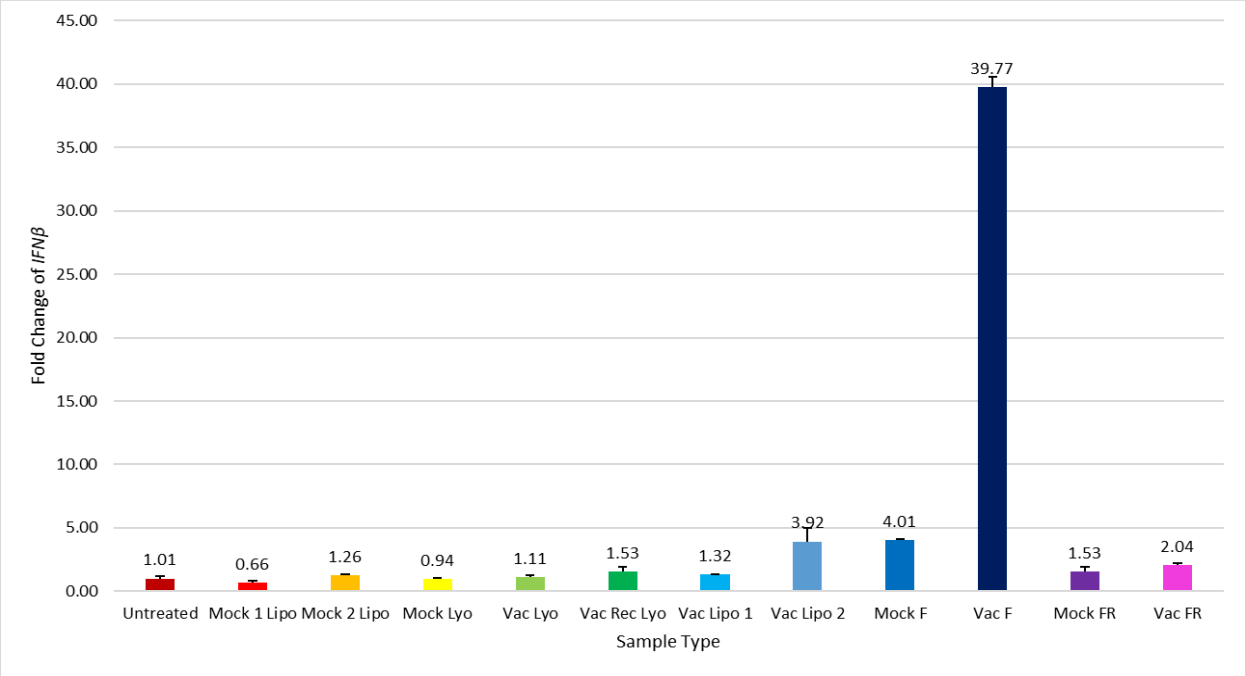

Figure 13: Transcription of *IFN*□ under untreated and various lipid transfected treatments. PMA-treated THP-1 cells stimulated with various lipid-based reagents including Lipofectamine with Opti-MEM. Measurements were taken 24 hours after stimulation. Data are representative of the mean of technical triplicates from three experiments, and error bars represent the standard deviation.

By integrating these procedural steps, we analyzed the transcriptional profiles of *IFNβ* and *ISG56* under four conditions: no transfection, Vac70 DNA transfection, lipid-only transfection, and mtDNA release drugs. The data revealed that both DNA transfection and the mtDNA release drugs significantly increased *IFNβ* gene expression relative to unstimulated samples (Figure 14). Parallel transcription patterns were observed for *ISG56* under the same experimental conditions (Figure 15). Interestingly, lipid transfection alone also increased the transcription of both *IFNβ* and *ISG56* compared to the untreated negative control, suggesting that lipid delivery may induce cell stress.

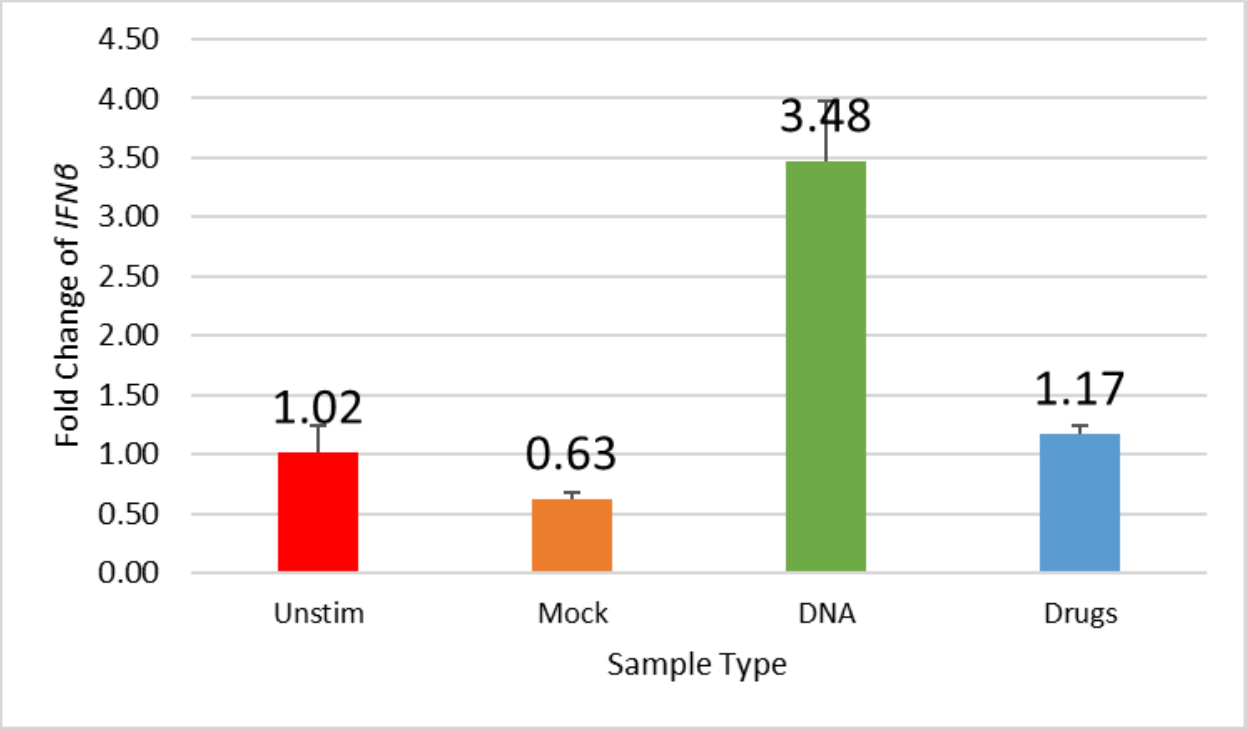

Figure 14: Transcription of IFN□ under untreated, lipid transfected, viral DNA, and positive control treatment. PMA-treated THP-1 cells stimulated with Vac70 DNA, Lipofectamine with Opti-MEM, and the positive controls (Q-VD-OPH and ABT-737). The negative control, also referred to as the untreated sample, consisted of cells receiving no stimuli. Measurements were taken 24 hours after stimulation. Data are representative of the mean of technical triplicates from three experiments, and error bars represent the standard deviation.

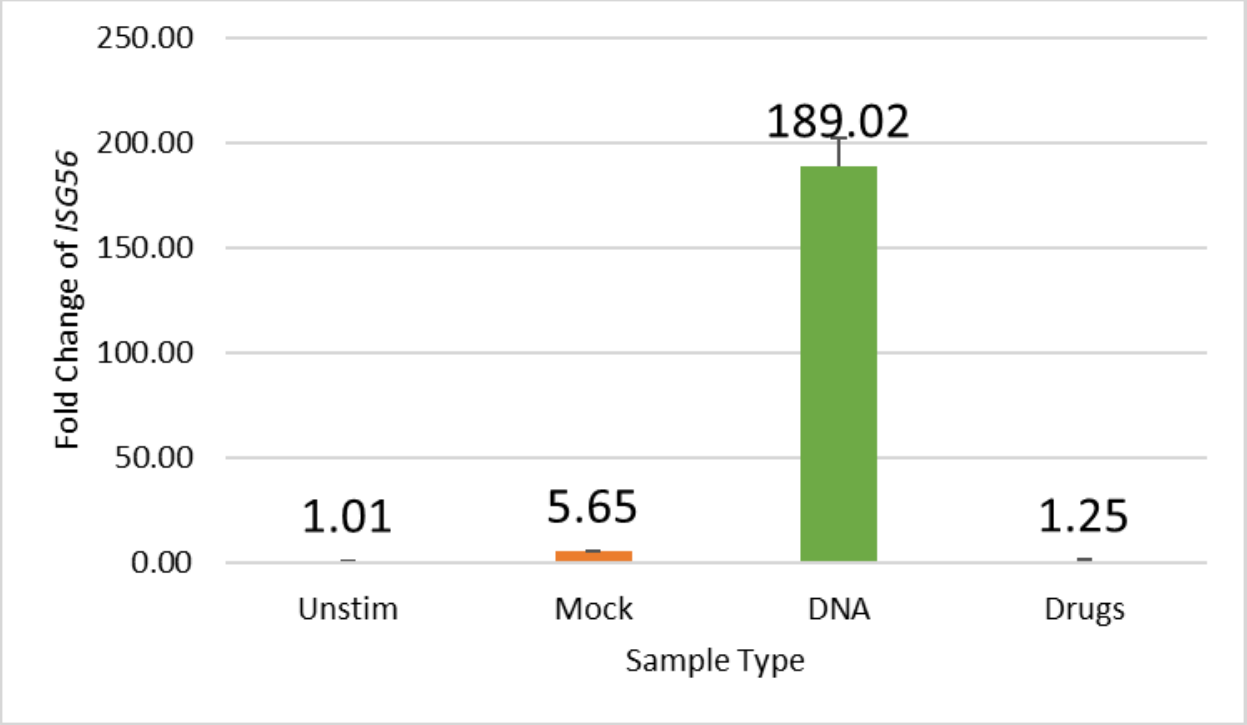

Figure 15: Transcription of *ISG56* under untreated, lipid transfected, viral DNA, and positive control treatment. PMA-treated THP-1 cells stimulated with Vac70 DNA, Lipofectamine with Opti-MEM, and the positive controls (Q-VD-OPH and ABT-737). The negative control, also referred to as the untreated sample, consisted of cells receiving no stimuli. Measurements were taken 24 hours after stimulation. Data are representative of the mean of technical triplicates from three experiments, and error bars represent the standard deviation.

Discussion

The objective of this study is to advance our understanding of the cGAS-STING pathway when viral DNA is present. Studies have shown that viral RNA infections indirectly activate the cGAS-STING pathway through the induction of cellular stress and mtDNA leakage (Hu et al., 2023). Given that RNA viruses trigger mtDNA leakage in addition to viral genome recognition, we hypothesize that DNA viruses employ a parallel mechanism where mtDNA is partially responsible for cGAS-STING activation. Viral DNA may induce cellular stress that triggers a secondary release of mtDNA. This study therefore tests the hypothesis that mtDNA, rather than viral DNA itself, is responsible for cGAS-STING activation during viral DNA infections. To test this hypothesis, mtDNA leakage was experimentally modeled in THP-1 cells, followed by analysis of innate immune gene expression and DNA compartmentalization. THP-1 cells were treated with ABT-737 and Q-VD-OPH–two drugs that have been confirmed to induce cellular stress and promote mtDNA release while inhibiting apoptosis. Transcriptional responses of *IFNβ* and *ISG56* were assessed through qPCR across four treatment groups: untreated, mock-transfected, viral DNA-stimulated, and drug-treated cells. At the same time, an adapted DNA fractionation protocol was used to isolate and quantify nuclear, cytosolic, and mitochondrial DNA (Bryant et al. 2022). Our findings partially support the hypothesis by demonstrating a link between mtDNA leakage and the upregulation of the cGAS-STING immune response. Specifically, we successfully induced and quantified mtDNA leakage via qPCR, suggesting a significant increase in *IFNβ* and *ISG56* expression. While this confirms the activation of the signaling pathway, further research is required to differentiate whether the transcriptional response during viral infection is driven primarily by the leaked mtDNA or the viral DNA itself.

Viral DNA and mtDNA Leakage Resulted in Increased *IFN□ and ISG56* Expression

Before any conclusions can be drawn regarding the predominant trigger for cGAS-STING activation, it must be clear that the stimuli of interest results in transcriptional upregulation of the innate genes of interest: *IFN□* and *ISG56.* RNA extraction, cDNA synthesis, and RT-qPCR results confirm that both types of DNA, viral and mtDNA, alongside lipid transfection increased the expression of *IFNβ* (Figure 14) and *ISG56* (Figure 15). The effects of viral DNA and the mtDNA release drugs were expected based on current literature (Bryant et al. 2022). *ISG56* is one of the many genes activated by Type I IFNs; therefore, an increase in *IFN□* expression explains an increase in *ISG56*. Furthermore, results from the 48-hour kinetics experiment indicate that the optimal time for stimulation and transcriptional analysis of *IFNβ* expression is between 6–18 hours (Figure 7), while *ISG56* expression is best analyzed at a later window between 12–24 hours (Figure 8). These time frames correlate with literature in the field. *ISG56* is a type of gene activated by interferons, which needs to occur rapidly to signal the body's innate immune system to fight infections through the "antiviral state" (West et al. 2015). The comparison between expression of *IFNβ* (Figure 9) and *ISG56* (Figure 10) after 24 hours versus 48 hours revealed higher expression levels of *IFNβ* at 24 hours, an earlier time point, and *ISG56* at 48 hours, a later time point. The presence of ISGs and Type I IFNs are generally indicative of an innate immune response. This suggests that mtDNA, alongside viral DNA, can activate a viral immune response – presumably through a cGAS-STING pathway.

Adverse Effects of Lipid Transfection: Possible mtDNA Leakage

An unexpected finding emerged early in the study: lipid transfection alone significantly increased the expression of *IFNβ* and *ISG56* compared to untreated samples (Figures 7 and 8). Our lab's standard protocol utilizes a liposomal-based transfection reagent, in which a mixture of Lipofectamine and Opti-MEM enables a lipid to merge with the phospholipid bilayer of the host cell to allow the entry of the foreign genetic materials with minimal resistance (Kim and Eberwine 2010). At the time, the lipid ("mock") was acting as the negative control rather than the untreated. When taking a closer look at the mock samples, there was an unexpected increase of innate gene expression. While it is recognized that lipid transfection is a suboptimal negative control, the underlying mechanism and explanation remained unclear. Our lab hypothesizes that mtDNA leakage may be possible due to the lipid prompting cellular stress and thus, mtDNA leakage. To support this conclusion, one must measure whether mtDNA is being released. When compartmentalizing and extracting mtDNA from the whole cell versus the cytosol, there was an increase in DNA found in the cytosol during lipid transfection – most obviously seen in Figure 6. Future investigations could look for a relationship between lipid transfection and mtDNA release as was done in our analysis of 9 other lipid reagents. There was a minimal to major increase in increased expression of *IFNβ* (Figure 13) when we conducted this assay and from this point on, untreated samples acted as negative controls to avoid any adverse mtDNA leakage. These results supply an explanation for adverse effects induced by lipid transfection in immunological studies.

Procedures for Compartmentalizing and Extracting mtDNA

The methodology in this study was adapted from previously existing and published research (Bryant et al. 2022). However, this was the first time these procedures were replicated at

Drew University and most importantly: successfully. Our treatment types, as revealed in Figure 5 and 6, indicate that the various stimuli do not change the overall amount of mtDNA in the entire cell. Any discrepancy, specifically the decrease in DNA after the positive drug combination (Figure 5), may be due to DNA released into the cytosol and then degraded. To conclude whether the discrepancy in the drug treatment is due to degradation, a cytotoxicity test must be conducted as it can indicate DNA damage and degradation. It is important to recognize that cytotoxicity itself, cell death or membrane damage, can cause DNA damage-like-breaks that look like genotoxicity. It is essential that specialized assays are equipped to distinguish between genotoxicity (direct DNA damage) and cytotoxicity (secondary DNA damage from cell death). While possibly toxic and lethal to the cells, these drugs (as supported by the literature) cause leakage of mtDNA into the cytosol, which was expected based on the literature. The more important novel discovery, as indicated best by Figure 6, is that viral DNA mediates mtDNA leakage albeit not as high as the drug combination. How this is possible was not determined in this study but warrants further research on the matter.

Future Direction and Broader Implications

To further understand how cells detect mtDNA during a viral DNA infection, it is critical to assess whether viral or mtDNA triggers the cGAS-STING pathway. While Figure 5 and 6 show mtDNA release during viral DNA stimuli, they do not fully address our hypothesis. Thus, the logical next step would be to design an experiment that indicates viral DNA infections stimulating mtDNA leakage and that the mtDNA leakage is what activates the antiviral state rather than the DNA from the virus alone. If a specific experimental treatment like viral DNA or the positive control drugs leads to an increase in transcription of *IFNβ* or *ISG56* and higher

mtDNA levels, this would suggest more clearly that viral infection drives mtDNA leakage. Moreover, mtDNA leakage transcriptionally upregulates innate gene expression and, as a result, activates the antiviral state via the cGAS-STING pathway (Figure 16). Figure 17 represents the alternative: viral DNA itself increases gene expression and mtDNA leakage, but it is the viral DNA that is responsible for activation of the cGAS-STING pathway.

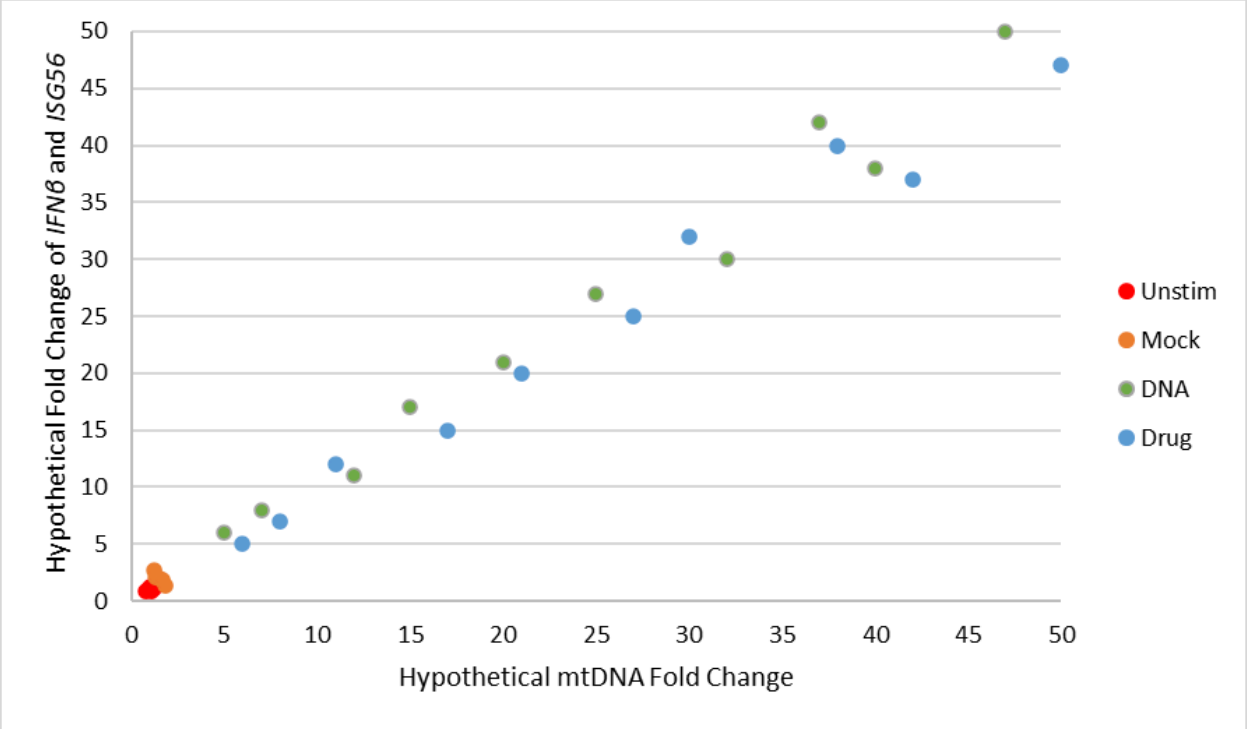

Figure 16: Hypothetical Future Study Results if gene expressions are mediated through mtDNA leakage. This hypothetical diagram depicts a scatter plot with horizontal axis (mtDNA presence and load) while the vertical axis would have IFNβ and ISG56 expression. The proposed experiment would follow a similar methodology, including 4 experimental conditions (unstimulated, mock, DNA and drugs).

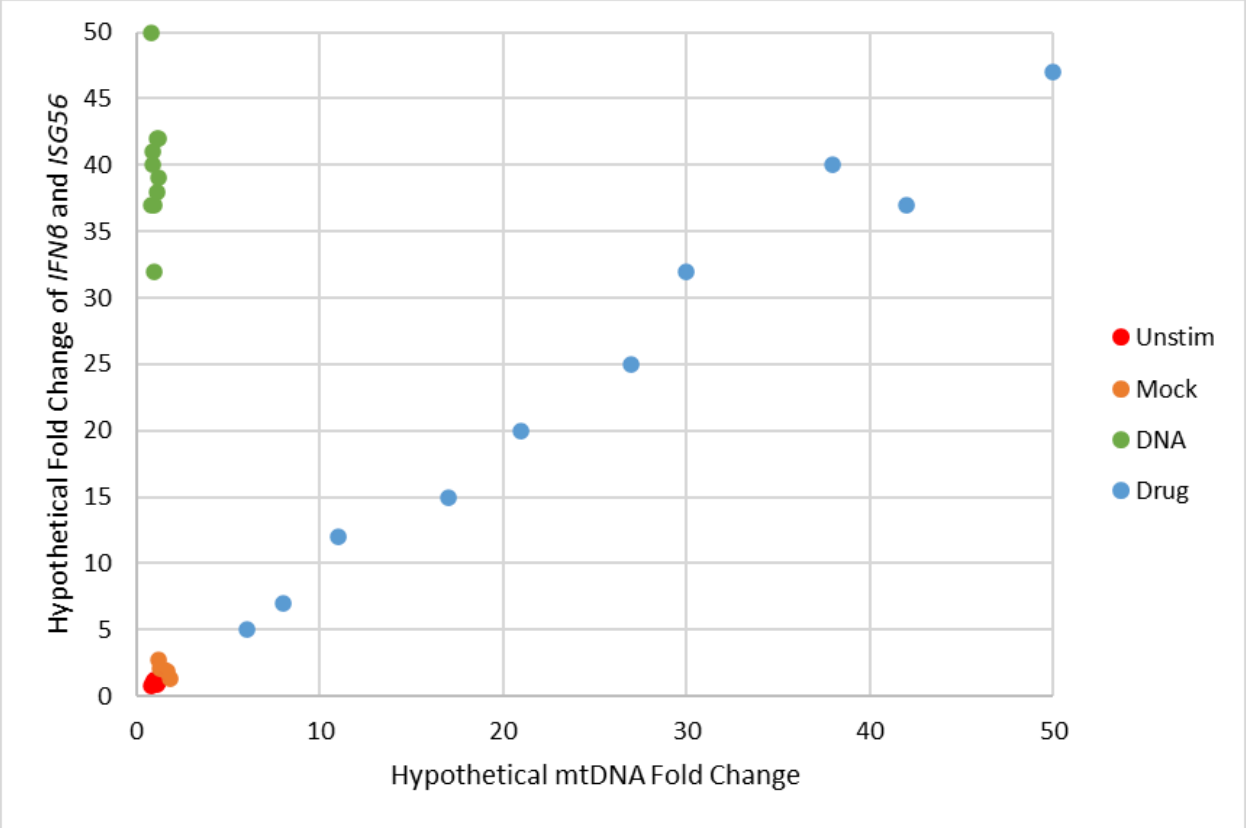

Figure 19: Hypothetical future study results if gene expression is mediated through viral DNA itself. This hypothetical diagram depicts a scatter plot with horizontal axis (mtDNA presence and load) while the vertical axis would have IFNβ and ISG56 expression. The proposed experiment would follow a similar methodology, including 4 experimental conditions (unstimulated, mock, DNA and drugs).

Another possible route of study is further examining the cGAS-STING pathway itself. This study is based on the hypothesis that during a viral DNA infection, the cGAS-STING pathway is sensing viral DNA mediated mtDNA leakage. To further understand mechanistically, CRISPR knockout cell lines targeting *STING*, *cGAS*, and *IFI16* could be used to identify the key genes involved in mtDNA-mediated immune activation. If stimulation with the two positive control drugs fails to induce innate immune products in the specific knockout cell line, then the targeted gene would be considered central to the cGAS-STING pathway.

The potential of this study and the adapted protocols (Bryant et al. 2022) is endless. The correlation between mtDNA, inflammation, and possibly autoimmune disease have been proposed throughout the field. These protocols, alongside Q-VD-OPH and ABT-737, would allow researchers to expand into areas of research and experiments that will allow for further understanding of the systems of immune activation and regulation.

References

Aguirre S, Luthra P, Sanchez-Aparicio MT, Maestre AM, Patel J, Lamothe F, Fredericks AC, Tripathi S, Zhu T, Pintado-Silva J, Webb LG, Bernal-Rubio D, Solovyov A, Greenbaum B, Simon V, Basler CF, Mulder LC, García-Sastre A, Fernandez-Sesma A. 2017. Dengue virus NS2B protein targets cGAS for degradation and prevents mitochondrial DNA sensing during infection. Nature Microbiology. 2:17037. doi:10.1038/nmicrobiol.2017.37.

Amurri L, Horvat B, Iampietro M. 2023. Interplay between RNA viruses and cGAS/STING axis in innate immunity. Front Cell Infect Microbiol. 13:1172739. https://doi.org/10.3389/fcimb.2023.1172739.

Bryant JD, Lei Y, VanPortfliet JJ, Winters AD, West AP. 2022. Assessing mitochondrial DNA release into the cytosol and subsequent activation of innate immune-related pathways in mammalian cells. Curr Protoc. 2(2):e372. doi:10.1002/cpz1.372.

Hu MM, Shu HB. 2023. Mitochondrial DNA-triggered innate immune response: mechanisms and diseases. Cell Mol Immunol. 20(12):1403–1412. doi:10.1038/s41423-023-01082-x.

Jahun AS, Sorgeloos F, Chaudhry Y, Arthur SE, Hosmillo M, Georgana I, Izuagbe R, Goodfellow IG. 2023. Leaked genomic and mitochondrial DNA contribute to the host response to noroviruses in a STING-dependent manner. Cell Rep. 42(3):112179. doi:10.1016/j.celrep.2023.112179.

Kanneganti TD, Kundu M, Green DR. 2015. Innate immune recognition of mtDNA--an undercover signal?. Cell Metab. 21(6):793–794. doi:10.1016/j.cmet.2015.05.019.

Kim TK, Eberwine JH. 2010. Mammalian cell transfection: the present and the future. Anal Bioanal Chem. 397(8):3173–3178. doi:10.1007/s00216-010-3821-6.

Lang BF, Gray MW, Burger G. 1999. Mitochondrial genome evolution and the origin of eukaryotes. Annu Rev Genet. 33:351-397. doi:10.1146/annurev.genet.33.1.351.

Maess MB, Sendelbach S, Lorkowski S. 2010. Selection of reliable reference genes during THP-1 monocyte differentiation into macrophages. BMC Mol Biol. 11:90. doi:10.1186/1471-2199-11-90.

Mogensen TH. 2009. Pathogen recognition and inflammatory signaling in innate immune defenses. Clin Microbiol Rev. 22(2):240–273. doi:10.1128/CMR.00046-08.

Parham P. 2021. The immune system. 5th ed. New York (NY): W. W. Norton & Company.

Popovici V, Goldstein DR, Antonov J, Jaggi R, Delorenzi M, Wirapati P. 2009. Selecting control genes for RT-QPCR using public microarray data. BMC Bioinformatics. 10(42):1-10. doi:10.1186/1471-2105-10-42.

Tsuchiya S, Yamabe M, Yamaguchi Y, Kobayashi Y, Konno T, Tada K. 1980. Establishment and characterization of a human acute monocytic leukemia cell line (THP-1). Int J Cancer. 26(2):171-176. doi:10.1002/ijc.2910260208.

Unterholzner L, Keating S, Baran M, Horan K, Jensen S, Sharma S, Sirois C, Jin T, Latz E, Xiao S, et al. 2010. IFI16 is an innate immune sensor for intracellular DNA. Nat Immunol. 11(11):997–1004. doi:10.1038/ni.1932.

VanPortfliet JJ, Chute C, Lei Y, Shutt TE, West AP. 2024. Mitochondrial DNA release and sensing in innate immune responses. Hum Mol Genet. 33(R1):R80–R91. doi:10.1093/hmg/ddae031.

West AP, Shadel GS. 2017. Mitochondrial DNA in innate immune responses and inflammatory pathology. Nat Rev Immunol. 17(6):363–375. doi:10.1038/nri.2017.21.

West AP, Khoury-Hanold W, Staron M, Tal MC, Pineda CM, Lang SM, Bestwick M, Duguay BA, Raimundo N, MacDuff DA, et al. 2015. Mitochondrial DNA stress primes the antiviral innate immune response. Nature. 520(7548):553–557. doi:10.1038/nature14156.

Xia L, Yan X, Zhang H. 2025. Mitochondrial DNA-activated cGAS-STING pathway in cancer: Mechanisms and therapeutic implications. Biochim Biophys Acta Rev Cancer. 1880(1):189249. doi:10.1016/j.bbacan.2024.189249.

Yoh SM, Schneider M, Seifried J, Soonthornvacharin S, Akleh RE, Olivieri KC, De Jesus PD, Ruan C, de Castro E, Ruiz PA, et al. 2015. PQBP1 is a proximal sensor of the cGAS-dependent innate response to HIV-1. Cell. 161(6):1293–1305. doi:10.1016/j.cell.2015.04.050.